Ab initio study on the electronic states and laser cooling of AlCl and AlBr

Rong Yang(杨荣)[1,2], Bin Tang(唐斌)[3], and Tao Gao(高涛)[2,†]

[1] *College of Materials Science and Engineering, Chongqing Jiaotong University, Chongqing* 400074, *China*
[2] *Institute of Atomic and Molecular Physics, Sichuan University, Chengdu* 610065, *China*
[3] *Institute of Finance & Trade, Chongqing City Management College, Chongqing* 401331, *China*

(Received 26 September 2015; revised manuscript received 29 December 2015; published online 20 February 2016)

We investigate whether AlCl and AlBr are promising candidates for laser cooling. We report new *ab initio* calculations on the ground state $X^1\Sigma^+$ and two low-lying states ($A^1\Pi$ and $a^3\Pi$) of AlCl and AlBr. The calculated spectroscopic constants show good agreement with available theoretical and experimental results. We also obtain the permanent dipole moments (PDMs) curve at multi-reference configuration interaction (MRCI) level of theory. The transition properties of $A^1\Pi$ and $a^3\Pi$ states are predicted, including the transition dipole moments (TDMs), Franck–Condon factors (FCFs), radiative times and radiative width. The calculated radiative lifetimes are of the order of a nanosecond, implying that they are sufficiently short for rapid laser cooling. Both AlCl and AlBr have highly diagonally distributed FCFs which are crucial requirement for molecular laser cooling. The results demonstrate the feasibility of laser cooling AlCl and AlBr, and we propose laser cooling schemes for AlCl and AlBr.

Keywords: AlCl, AlBr, laser cooling

PACS: 31.15.A–, 37.10.Mn, 87.80.Cc **DOI:** 10.1088/1674-1056/25/4/043101

1. Introduction

Ultracold molecules offer a unique opportunity for studying chemical reactions at the quantum state level. Recently, the laser cooling of diatomic molecules has been demonstrated in the laboratory.[1–3] It is notable that molecule SrF[1] has been directly cooled by Doppler and Sisyphus cooling for the first time. Later YO[2] and CaF[3] have also been experimentally cooled by laser cooling. It would be good to note that similar schemes have now been proposed for molecular ions (eg the molecular hydrogen ions[4] HD^+). The researches on the laser cooling in our country are also motivated by all sorts of prospective applications.[5–7] Since there are more than 90 elements in the periodic table, it may form more than 4000 different diatomic molecules. Naturally the search for potential laser cooling candidates is getting people to pay attention. For laser cooling of a molecule, it is very difficult to keep a closed optical pumping cycle with repeated optical spontaneous emissions due to the molecule's complex internal structure. SrF, YO, and CaF all demonstrate highly-diagonal Franck–Condon factors (FCFs) which suppress decays to unwanted sublevels. So in order to be a possible source for laser cooling, the molecule must meet the first criteria: highly-diagonal FCFs. The highly-diagonal FCFs would limit the number of lasers required to keep the molecule in a closed-loop cooling cycle. A second criteria is that rapid laser cooling calls for shorter lifetimes. SrF, YO, and CaF all have short lifetimes. The calculations of FCFs and lifetimes would help us to identify promising candidates for laser cooling theoretically. Thus, we use *ab initio* calculations to investigate the possibility of laser cooling AlCl and AlBr in this paper.

In 2004, a brief survey of laser cooling candidates was presented by Di Rosa.[8] The list of candidates included aluminum compounds. The laser cooling of the related diatomics AlH and AlF has been discussed in detail by Wells and Lane.[9] They identified AlH and AlF as suitable laser cooling candidates. Now we would like to choose the two molecules AlCl and AlBr, since they have large emission probability (thus high scattering rates), very low scattering probabilities into off-diagonal bands $0 \rightarrow 1$ and $0 \rightarrow 2$, the desirable $^1\Pi \leftarrow ^1\Sigma^+$ cycling transitions and extremely short excited state lifetimes.

Aluminum monohalides (AlCl and AlBr) are readily produced in the vapor phase by high temperature pyrolysis[10] and from chemiluminescent reactions[11] of Al atoms with the halogens. A high-resolution emission spectrum of AlCl at 20 μm was conducted by Hedderich *et al.*[12] They have found that the ground state $X^1\Sigma^+$ of AlCl possesses a deep potential. The previous experimental studies of electronic excited states for AlCl consisted mainly of absorption and emission spectra from the first singlet–singlet (i.e. A–X), triplet–triplet (b–a) and triplet–singlet (a–X) systems.[12–18] Theoretical calculations have also been performed for AlCl over the past several decades. For AlCl, the potential curves for the $X^1\Sigma^+$ and $A^1\Pi$ states, and $A^1\Pi$ vibrational lifetimes were given by Langhoff

†Corresponding author. E-mail: gaotao@scu.edu.cn

© 2016 Chinese Physical Society and IOP Publishing Ltd

et al.[19] Brites *et al.*[20] obtained the lifetime of AlCl for the $A^1\Pi v' = 0$ level of 5.9 ns. These authors all agreed that AlCl has highly-diagonal FCFs and short radiative lifetimes. Several experimental and theoretical studies of the AlBr molecule are also available. Bredohl *et al.*[21] have provided an extensive high-resolution band-by-band analysis of 28 bands of the A–X transition of AlBr. The $A^1\Pi$–$X^1\Sigma^+$ transition of AlBr was recorded by Fleming *et al.*[22] using a Bruker IFS 120 HR Fourier transform spectrometer. Their results showed that the 0–0 band was the most intense and the $\Delta v = 0$ sequence dominated the observed spectrum. Recent theoretical calculations have been performed for 12 electronic states for AlBr by Hamade *et al.*[23] The radiative lifetime for the $v' = 0$ level of the $A^1\Pi$ state was computed by Langhoff *et al.*[19] to be about 8.5 ns for AlBr using averaged complete active space self-consistent field (CASSCF)[24,25] calculations.

As stated above, AlCl and AlBr have been researched systematically. Nevertheless, systematic studies of laser cooling of AlCl and AlBr are not available in the literature. So our work focuses on identifying whether AlCl and AlBr are possible candidates for laser cooling with *ab initio* calculations. Because AlCl and AlBr both possess $^1\Pi \leftarrow {}^1\Sigma^+$ transition, the FCFs, transition dipole moments (TDMs), radiative lifetimes and radiative widths of the $A^1\Pi$–$X^1\Sigma^+$ transtions of AlCl and AlBr are predicted. Also accurate determinations of the spectroscopic constants, potential energy curves (PECs) and permanent dipole moments (PDMs) of the $X^1\Sigma^+$ and $A^1\Pi$ states of AlCl and AlBr have been given. Additionally, there is a low lying $a^3\Pi$ state between the $A^1\Pi$ and ground states for AlCl and AlBr. The PECs, spectroscopic constants of $a^3\Pi$ state, and the transition properties of the $a^3\Pi$ state to the ground state are also obtained. Finally, we briefly design laser cooling schemes for AlCl and AlBr.

The present paper is organized as follows. In Section 2 we give the details of our calculations. Section 3 presents the results and discussion, outlining laser cooling schemes for AlCl and AlBr. The conclusions are summarized in Section 4.

2. Computational method

All our *ab initio* calculations are performed using the MOLPRO package.[26] The ground state ($X^1\Sigma^+$) and two low-lying excited states ($A^1\Pi$ and $a^3\Pi$) for AlCl and AlBr have been conducted with multi-reference configuration interaction (MRCI) plus Davidson corrections[27–29] which is based on CASSCF[24,25] wave functions. For AlBr, the scalar relativistic effects are taken into account using the Douglas–Kroll–Hess[30,31] transformation of the relativistic Hamiltonian. The spectroscopic constants (R_e, D_e, w_e, $w_e\chi_e$, B_e, T_e) are derived by using Le Roy's LEVEL 8.0 program.[32] The PDMs and TDMs of AlCl and AlBr are evaluated by taking the expectation and transition values using the MRCI wave functions. Spin–orbit coupling is ignored in our calculations, since the principal transitions under investigation are singlet states.

In our calculations, the basis sets aug-cc-PVQZ[33] are used for Al and Cl. As for Br, we choose the small-core scalar relativistic effective core potential ECP10MDF[34] together with the corresponding valence basis sets.[35] Owing to the limitation of the MOLPRO software package, C_{2v} point group symmetry has been considered for AlCl and AlBr in all computations, which holds (a_1, b_1, b_2, a_2) irreducible representations. For AlCl, eight molecule obitals (MOs) are put into active space, including four a_1, two b_1, two b_2 symmetry MOs (4220), which correspond to the 3s3p shells of the Al atom and 3s3p shells of the Cl atom. The active space of AlBr consists of eight MOs $4a_1$, $2b_1$, $2b_2$, $0a_2$ (4220) which correspond to Al 3s3p and Br 4s4p.

3. Results

3.1. PECs and spectroscopic constants

Figure 1 shows the PECs of the ground state ($X^1\Sigma^+$) and two low-lying excited states ($A^1\Pi$ and $a^3\Pi$) of AlCl and AlBr obtained at the MRCI level of theory. We summarize the corresponding spectroscopic constants in Table 1. Previous experimental and theoretical data are listed together.

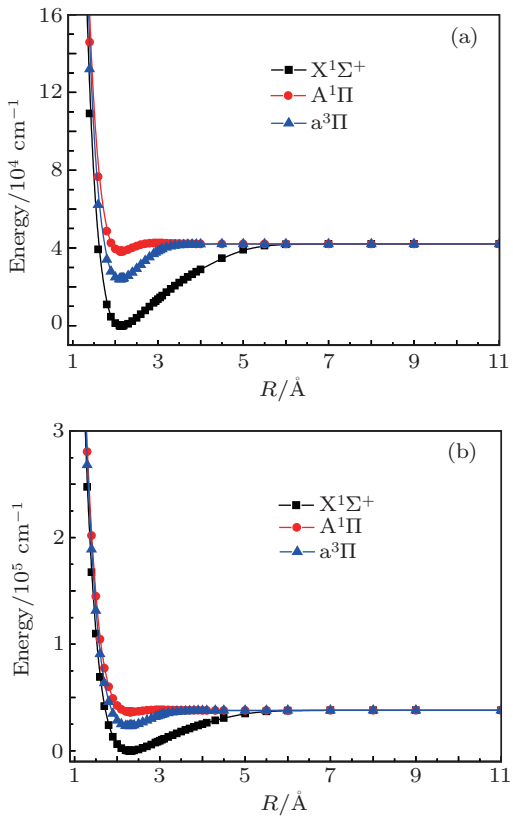


Fig. 1. (color online) Potential energy curves of the first three electronic states of AlCl (a) and AlBr (b) at the MRCI level of theory.

Table 1. Calculated spectroscopic constants of $X^1\Sigma^+$, $A^1\Pi$, and $a^3\Pi$ states of AlCl and AlBr at the MRCI level of theory.

Molecule	States	T_e	R_e/Å	w_e/cm^{-1}	$w_e\chi_e$/cm^{-1}	B_e	D_e	Ref.
AlCl	$X^1\Sigma^+$	0	2.145	478.36	1.95	0.2406	5.22	this work
		0	2.130	481.70	2.07	0.2439	5.25±0.01[a]	Exp[35]
		–	2.140	484.50	6.47	0.2418	–	Ref. [20]
	$A^1\Pi$	38303	2.142	471.83	9.61	0.2412	0.53	this work
		38254	2.124[b]	449.96	–	–	–	Exp[37]
		–	2.132	453.00	8.03	0.2435	–	Ref. [20]
	$a^3\Pi$	24057	2.112	523.36	2.61	0.2481	2.24	this work
		–	2.100	524.35	2.18	0.2500	–	Exp[17]
		–	2.107	519.10	0.52	0.2494	–	Ref. [20]
AlBr	$X^1\Sigma^+$	0	2.306	378.72	1.20	0.1577	4.71	this work
		0	2.295[c]	378.11	1.31	0.1592	4.40[c]	Exp[20]
		–	2.317	377.00	–	–	4.52	Ref. [17]
	$A^1\Pi$	36418	2.325	314.59	7.61	0.1551	0.24	this work
		35880	2.322[c]	296.16	5.68	0.1548[d]	–	Exp[22]
		36450	2.337	316.00	–	–	–	Ref. [19]
	$a^3\Pi$	23308	2.263	409.46	1.72	0.1637	1.81	this work
		23778	–	410.30	1.72	0.1651	–	Exp[38]

[a] Refs. [14] and [36]; [b] Ref. [36]. [c] Ref. [37]. [d] Ref. [38].

For AlCl, our results are close to the experimental data. The percentage error in R_e, w_e, and $w_e\chi_e$ are 0.70%, 0.69%, and 5.80% for the ground state $X^1\Sigma^+$ of AlCl. Findings for the excited state $a^3\Pi$ of AlCl are similar; the percentage error in R_e, w_e, and $w_e\chi_e$ are 0.57%, 0.19%, and 19.72% compared with the experimental data.[17] Although the deviation of the $w_e\chi_e$ seems to be a little large, our calculated values are closer to the experimental data[17,35] than the theoretical results obtained by Brites *et al.*[20] The percentage error in $w_e\chi_e$ calculated by Brites *et al.*[20] are 212.56% and 76.09% for the $X^1\Sigma^+$ and $a^3\Pi$ states of AlCl. The computed ground state dissociation energy D_e of 5.22 eV compares well with the experimental value of (5.25±0.01) eV.[14,36] Our calculated T_e result is only 49 cm^{-1} larger than the observed data[37] for the $A^1\Pi$ state of AlCl.

We turn now to the discussion of AlBr. Our calculated spectroscopic constants of AlBr are also close to the experimental values, compared with previous theoretical data obtained by Langhoff *et al.*[19] The calculated R_e, w_e, and B_e for $X^1\Sigma^+$ state of AlBr are 2.306 Å, 378.72 cm^{-1} and 0.1577 cm^{-1} respectively, which are in good agreement with the experimental data 2.295 Å, 378.11 cm^{-1}, and 0.1592 cm^{-1}. For the $A^1\Pi$ state of AlBr, the percentage error in T_e, R_e, and w_e are 1.50%, 0.13%, and 6.22% compared with the experimental data,[22] and for the $a^3\Pi$ states of AlBr, the percentage error in T_e, w_e, and $w_e\chi_e$ are 1.98%, 0.20%, and 0.29%.

Overall, our computed spectroscopic constants agree well with the experimental data as well as other available theoretical results. We expect that our methods are accurate for the two molecules.

3.2. PDMs and TDMs

Figures 2 and 3 show the PDMs of the $X^1\Sigma^+$ and $A^1\Pi$ states of AlCl and AlBr as functions of the internuclear distance at the MRCI level, respectively. A study of Fig. 2 reveals that at short bond lengths the dipole of each molecule possesses an essentially linear dependence

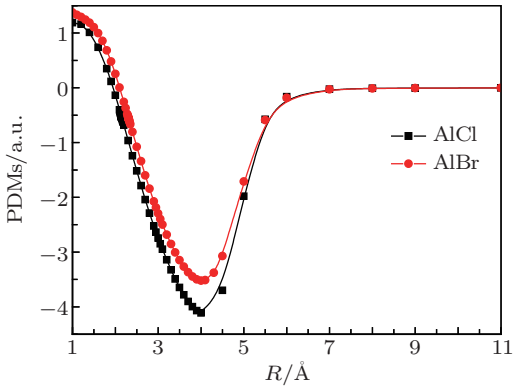


Fig. 2. (color online) PDMs of $X^1\Sigma^+$ state at the MRCI level for AlCl and AlBr.

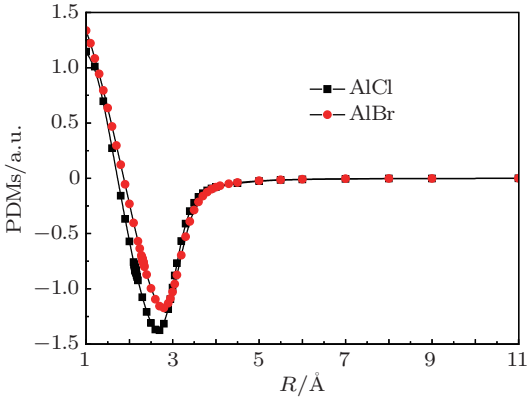


Fig. 3. (color online) PDMs of $A^1\Pi$ state at the MRCI level for AlCl and AlBr.

with the increase of the internuclear distance indicative of an ionic molecule. The absolute magnitude reaches a maximum (AlCl: −4.11 a.u. (the unit a.u. is short for atomic unit), AlBr: −3.52 a.u.) and drops thereafter. The dipole falls to zero at around 7 Å for both molecules. As shown in Fig. 3, the PDMs of the $A^1\Pi$ state demonstrate similar behavior as the PDMs of the $X^1\Sigma^+$ state. The peaks of the PDMs are −1.38 a.u. and −1.17 a.u. for AlCl and AlBr, respectively.

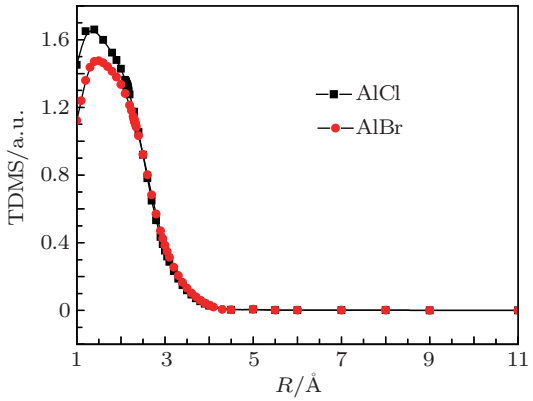


Fig. 4. (color online) TDMs for the transitions from the $A^1\Pi$ state to the $X^1\Sigma^+$state at MRCI level of AlCl and AlBr.

The relationship between the TDMs of the $A^1\Pi$–$X^1\Sigma^+$ transitions and the internuclear distance is depicted in Fig. 4. For AlCl and AlBr, the TDMs show similar behavior. The magnitude gradually increases as internuclear distance R increases, reaches a maximum (AlCl: 1.66 a.u., AlBr: 1.47 a.u.), and drops thereafter.

3.3. Radiative lifetime and radiative width

Rapid laser cooling requires sufficiently short lifetimes, which can provide a significant rate (10^5 s^{-1}–10^8 s^{-1}) of optical cycling. The radiative lifetimes and radiative width for the transitions from the $A^1\Pi$ state to the ground state $X^1\Sigma^+$ are collected in Table 2. The other theoretical results[19] are also listed in Table 2 for comparison. Table 2 shows that in all cases the lifetimes increase slowly with the vibrational quantum number. For AlCl, our computed lifetime for the $A^1\Pi$ $v' = 0$ level of 5.04 ns is close to the experimental value of (6.4±2.5) ns determined by Rogowski and Fontijn.[39] For AlBr, our value for the $v' = 0$ level of 8.53 ns also agrees with the theoretical value of 8.5 ns estimated by Langhoff *et al.*[19]

Table 2. Estimated radiative lifetimes (in unit ns) and radiative width (in unit cm^{-1}) (in italics) for $A^1\Pi \rightarrow X^1\Sigma^+$ transitions. Theoretical values obtained by Langhoff *et al.* in brackets.

Molecule	Transition	$v' = 0$	1	2	3	4
AlCl	$A^1\Pi \rightarrow X^1\Sigma^+$	5.04 (5.17)[a] *10.51(–4)*	5.19 (5.28)[a] *10.21(–4)*	5.35 (5.40)[a] *9.90(–4)*	5.54 (5.55)[a] *9.56(–4)*	5.76 (5.73)[a] *9.20(–4)*
AlBr	$A^1\Pi \rightarrow X^1\Sigma^+$	8.53 (8.5)[a] *6.21(–4)*	8.93 – *5.93(–4)*	9.41 – *5.63(–4)*	10.00 – *5.29(–4)*	10.83 – *4.89(–4)*

[a)]Ref. [19]. [b)]Characteristic base 10 given parenthetically.

The radiative lifetimes of the $A^1\Pi(v')$ vibrational states are computed to be 5.04 ns–5.76 ns and 8.53 ns–10.83 ns for the first five vibrational levels ($v' = 0$–4) of AlCl and AlBr. So these lifetimes are sufficiently short that AlCl and AlBr meet the criteria as suitable laser cooling candidates. Taking the $v' = 0$ level as an example, the line strengths (Einstein A coefficients) of the $A^1\Pi(v' = 0)$ vibrational states for AlCl and AlBr are 1.98×10^8 s^{-1} and 1.17×10^8 s^{-1}, giving lifetimes of 5.04 ns and 8.53 ns (about 1/5 and 2/5 that of the transition in SrF). The radiative widths of the $a^3\Pi$ and $A^1\Pi$ vibrational states are predicted in Table 2 for AlCl and AlBr. In all cases, the radiative widths show a slight decrease with increasing v'.

3.4. FCFs and proposed laser cooling scheme

The calculated FCFs in AlCl for the transition $A^1\Pi \rightarrow X^1\Sigma^+$ are tabulated in Table 3. Langhoff *et al.*[19] did not give FCFs for $A^1\Pi \rightarrow X^1\Sigma^+$ transition in AlCl. But Einstein coefficients (A) were given ($A_{00} = 1.933 \times 10^8$ s^{-1}, $A_{11} = 1.891 \times 10^8$ s^{-1}, $A_{22} = 1.832 \times 10^8$ s^{-1}, $A_{33} = 1.735 \times 10^8$ s^{-1}) by them. Our calculated Einstein coefficients are the following: $A_{00} = 1.979 \times 10^8$ s^{-1}, $A_{11} = 1.921 \times 10^8$ s^{-1}, $A_{22} = 1.841 \times 10^8$ s^{-1} and $A_{33} = 1.716 \times 10^8$ s^{-1}. Thus, our results can be compared with the results obtained by Langhoff *et al.*[19] Of course, our calculated FCFs need to be confirmed by later experimental data. It can be seen that the determined FCFs of AlCl are highly diagonally ($f_{00} = 0.9993$, $f_{11} = 0.9960$, $f_{22} = 0.9819$, $f_{33} = 0.9419$). Highly-diagonal FCFs are desirable for laser cooling. The calculated $v' = 0 \rightarrow v = 0$ FCF (f_{00}) of 0.9993 (Table 3), is larger than that predicted in SrF ($f_{00} = 0.98$), thus it is sufficiently large to be potentially viable for cooling. On the basis of the calculated FCFs, we propose a two color laser cooling scheme. The main cooling transition is the transition $A^1\Pi$ ($v' = 0$) $\leftarrow X^1\Sigma^+$ ($v = 0$) using wavelength $\lambda_{00} = 261.2$ nm (Fig. 5(a)); the corresponding experimental value[37] is 261.5 nm. Because there is a

non-negligible probability of decay to the $X^1\Sigma^+$ ($v = 2$) state ($\approx 0.07\%$), a repumping laser can be tied to the $v' = 1 \leftarrow v = 2$ transition with $\lambda_{21} = 258.6$ nm. Decays to the $X^1\Sigma^+$ ($v = 3$) state occur with probability $\approx 10^{-6}$. Using the repump should result in $N_{\rm scat} = 1/f_{03+} > 10^6$ photons scattered before higher vibrational levels are populated. The required cooling wavelength is deep into the UVC range (UVC: 280–190 nm), where it is hard to produce continuous wave laser radiation. However, a frequency tripled Ti: sapphire laser should be capable of generating useful quantities of light at the wavelength (261.2 nm). It is also important to note that there is a low lying $a^3\Pi$ state between the two states ($A^1\Pi$ and $X^1\Sigma^+$) for AlCl. The intervening $a^3\Pi$ state could kill the cooling scheme based on the transition $A^1\Pi \leftarrow X^1\Sigma^+$, if the $a^3\Pi \leftarrow A^1\Pi$ transition depopulates the excited state. So far there has been no experimental observation of the $a^3\Pi \leftarrow A^1\Pi$ transition. The rate for the $A^1\Pi \rightarrow a^3\Pi$ transition should be very small. Also we have computed the FCFs for the $a^3\Pi \rightarrow X^1\Sigma^+$ transition, in order to see whether the $a^3\Pi \rightarrow X^1\Sigma^+$ transition is another option for laser cooling.

Table 3. The calculated FCFs $f_{v'v}$ of AlCl for $A^1\Pi(v') \rightarrow X^1\Sigma^+(v)$ and $a^3\Pi(v') \rightarrow X^1\Sigma^+(v)$ transitions. Characteristic base 10 given parenthetically.

	$v' = 0$	1	2	3	Transition
$v = 0$	0.9993	0.1157(–8)	0.7078(–3)	0.2539(–5)	$A^1\Pi \rightarrow X^1\Sigma^+$
	0.8845	0.1093	0.6088(–2)	0.1683(–3)	$a^3\Pi \rightarrow X^1\Sigma^+$
1	0.9677(–6)	0.9960	0.1699(–2)	0.2241(–2)	$A^1\Pi \rightarrow X^1\Sigma^+$
	0.1077	0.6786	0.1959	0.0171	$a^3\Pi \rightarrow X^1\Sigma^+$
2	0.7077(–3)	0.1285(–2)	0.9819	0.1180(–1)	$A^1\Pi \rightarrow X^1\Sigma^+$
	0.7496(–2)	0.1895	0.5076	0.2617	$a^3\Pi \rightarrow X^1\Sigma^+$
3	0.1197(–5)	0.2643(–2)	0.8600(–2)	0.9419	$A^1\Pi \rightarrow X^1\Sigma^+$
	0.3614(–3)	0.0211	0.2473	0.3678	$a^3\Pi \rightarrow X^1\Sigma^+$

Table 3 shows that the FCFs for the $a^3\Pi \rightarrow X^1\Sigma^+$ transition are still highly diagonal. Thus, a four colour laser cooling scheme for AlCl using the $a^3\Pi \rightarrow X^1\Sigma^+$ transition is shown in Fig. 5(b). The main cycling laser drives the $a^3\Pi$ ($v' = 0$) $\leftarrow X^1\Sigma^+$ ($v = 0$) transition at length 415.4 nm (visible violet region, the corresponding experimental value is 407.36 nm[18]). The $a^3\Pi$ ($v' = 0$) $\leftarrow X^1\Sigma^+$ ($v = 1$) transition as the first vibrational repump and the $a^3\Pi$ ($v' = 1$) $\leftarrow X^1\Sigma^+$ ($v = 2$) transition for the second repump are required to reclaim molecules falling from $v' = 0$ to $v = 1$ (FCF = 0.1077) and $v' = 1$ to $v = 2$ (FCF = 0.1895). Owing to the non-negligible $a^3\Pi$ ($v' = 1$) to $X^1\Sigma^+$ ($v = 3$) transition (FCF = 0.0211), a third repumping laser may be required on that transition. The relatively long lifetimes of the $a^3\Pi$ state can be exploited to reach a much lower Doppler temperature than possible on the $A^1\Pi \leftarrow X^1\Sigma^+$ transition. Considering that the 0–0 band of the $a^3\Pi \rightarrow X^1\Sigma^+$ transition of AlCl at 407.36 nm has been observed by Saksena *et al.*,[18] AlCl may first be cooled on the strong $A^1\Pi \leftarrow X^1\Sigma^+$ transition, then be further cooled on the weak $a^3\Pi \leftarrow X^1\Sigma^+$ transition. This is similar to the laser cooling of alkaline earth atoms.

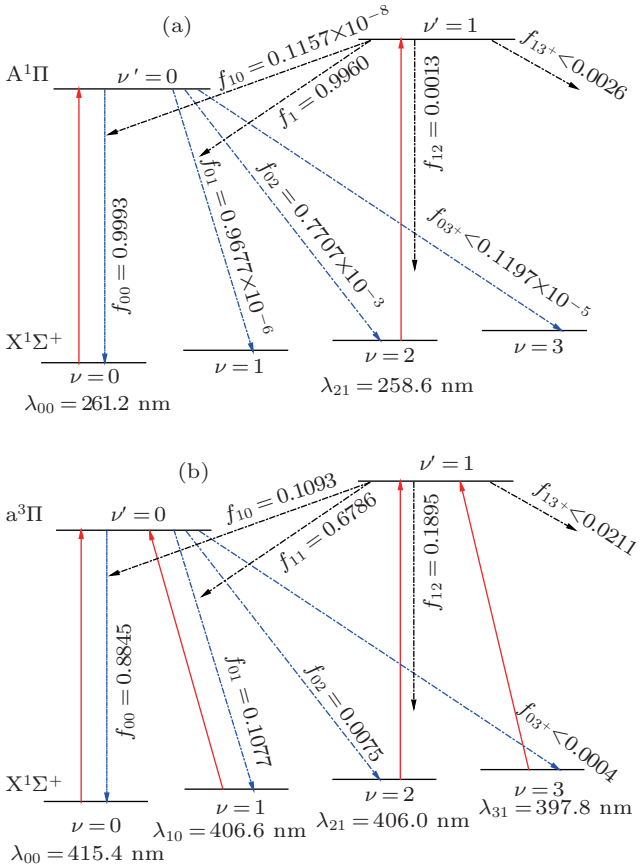


Fig. 5. (color online) Proposed laser cooling schemes for AlCl using the (a) $A^1\Pi(v') \leftarrow X^1\Sigma^+(v)$ and (b) $a^3\Pi(v') \leftarrow X^1\Sigma^+(v)$ transitions with the calculated FCFs $f_{v'v}$ and wavelength $\lambda_{v'v}$.

Turning to AlBr, the FCFs follow the same trend as that of AlCl (see Table 4). Although there are currently no experimental or theoretical data for FCFs of AlBr for comparison, our calculated wavelengths in Table 4 are close to the corresponding experimental values. The electronic spectrum of $A^1\Pi$–$X^1\Sigma^+$ and $a^3\Pi$–$X^1\Sigma^+$transitions were observed near 280 nm[38] and 420 nm.[38] As in AlCl, there is an $a^3\Pi$ state between $A^1\Pi$ and $X^1\Sigma^+$ states for AlBr. For simplicity, here we only propose laser cooling schemes of AlBr in Fig. 6.

On the whole, we have identified AlCl and AlBr as promising laser cooling candidates. Compared with AlBr ($f_{00} = 0.9371$), AlCl ($f_{00} = 0.9993$) is more promising. Because of the hyperfine structure present in Al diatomics, sub-Doppler sisyphus cooling can take place in AlCl and AlBr just like alkali atoms. For AlCl and AlBr, the $A^1\Pi \leftarrow X^1\Sigma^+$ transition may be followed by the weak $a^3\Pi \leftarrow X^1\Sigma^+$ transition. The recoil temperature ($T_{\rm recoil} = (h/\lambda)^2/2mk_{\rm B}$) is the temperature limitation. AlCl and AlBr have greater mass and cooling wavelengths of lower energy (AlCl: 415.4 nm; AlBr: 428.8 nm) than AlF investigated by Wells and Lane.[9] So the recoil temperature for AlCl and AlBr will be smaller than AlF.

Table 4. The calculated FCFs $f_{v'v}$ and wavelength $\lambda_{v'v}$ of AlBr for $A^1\Pi(v') \rightarrow X^1\Sigma^+(v)$ and $a^3\Pi(v') \rightarrow X^1\Sigma^+(v)$ transitions. Characteristic base 10 given parenthetically.

Transition	f_{00}	f_{10}	f_{01}	f_{11}	f_{02}	f_{12}	f_{03}	f_{13}	λ_{00}/nm	λ_{10}/nm	λ_{21}/nm	λ_{31}/nm
$A^1\Pi \rightarrow X^1\Sigma^+$	0.9371	0.0625	0.0532	0.7652	0.8622(–2)	0.1299	0.9358(–3)	0.0347	274.9	272.7	273.3	271.3
$a^3\Pi \rightarrow X^1\Sigma^+$	0.8085	0.1755	0.1681	0.5036	0.0212	0.2603	0.2047(–2)	0.0527	428.8	421.5	421.0	414.1

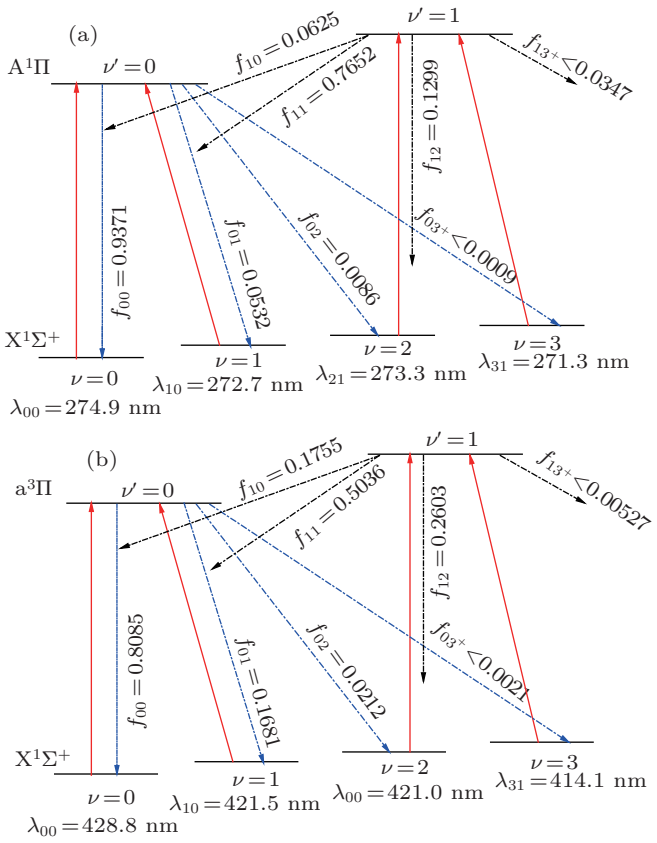


Fig. 6. (color online) Proposed laser cooling schemes for AlBr using the (a) $A^1\Pi(v') \leftarrow X^1\Sigma^+(v)$ and (b) $a^3\Pi(v') \leftarrow X^1\Sigma^+(v)$ transitions with the calculated FCFs $f_{v'v}$ and wavelength $\lambda_{v'v}$.

4. Conclusions

We have calculated the $X^1\Sigma^+$, $A^1\Pi$, and $a^3\Pi$ states of AlCl and AlBr in order to explore the possibility of laser cooling these molecules. First, we investigated the PECs and spectroscopic constants (R_e, D_e, w_e, $w_e\chi_e$, B_e, T_e). The calculated spectroscopic constants are in good agreement with previous theoretical and experimental data. Second, PDMs and TDMs have been calculated for the $X^1\Sigma^+$ and $A^1\Pi$ states. Finally, we obtained FCFs, radiative lifetimes and radiative widths. The results demonstrate that both molecules have highly diagonally distributed FCFs and short lifetimes. It means that AlCl and AlBr meet the criteria as promising candidates for direct laser cooling. Additionally, we have briefly designed laser cooling schemes for AlCl and AlBr. Since the $a^3\Pi \rightarrow X^1\Sigma^+$ transition is also strongly diagonal and the lifetimes of the excited $a^3\Pi$ state are relatively long, the $A^1\Pi \leftarrow X^1\Sigma^+$ transition may be followed by the weak $a^3\Pi \leftarrow X^1\Sigma^+$ transition to obtain a lower Doppler temperature.

Acknowledgments

The authors would like to thank Yufeng Gao for helpful comments and discussions.

References

[1] Shuman E S, Barry J F and DeMille D 2010 *Nature* **467** 820
[2] Hummon M T, Yeo M, Stuhl B K, Collopy A L, Xia Y and Ye J 2013 *Phys. Rev. Lett.* **110** 143001
[3] Zhelyazkova V, Cournol A, Wall T E, Matsushima A, Hudson J J, Hinds E A, Tarbutt M R and Sauer B E 2014 *Phys. Rev. A* **89** 053416
[4] Shen J, Borodin A, Hansen M and Schiller S 2012 *Phys. Rev. A* **85** 032519
[5] Wang Y Z 2011 *Physics* **40** 421 (in Chinese)
[6] Xu Z, Dang W R and Wang Y Z 2008 *Physics* **37** 708 (in Chinese)
[7] Zhou S Y, Long Q, Zhou S Y, Fu H X and Wang Y Z 2002 *Physics* **31** 481 (in Chinese)
[8] Di Rosa M D 2014 *Eur. Phys. J. D* **31** 395
[9] Wells N and Lane I C 2011 *Phys. Chem. Chem. Phys.* **13** 19018
[10] Dyke J M, Kirby C, Morris A, Gravenor B W J, Klein R and Rosrnus P 1984 *Chem. Phys.* **88** 289
[11] Rosenwaks S 1976 *J. Chem. Phys.* **65** 3668
[12] Hedderich H G, Dulick M and Bernath P F 1993 *J. Chem. Phys.* **99** 8363
[13] Mahanti P C 1934 *Z. Phys.* **88** 550
[14] Hildenbrand D L and Theard L P 1969 *J. Chem. Phys.* **50** 5350
[15] Mahieu E, Dubois I and Bredohl H 1989 *J. Mol. Spectrosc.* **134** 317
[16] Mahieu E, Dubois I and Bredohl H 1989 *J. Mol. Spectrosc.* **138** 264
[17] Sharma D 1951 *Astrophys. J.* **113** 210
[18] Saksena M D, Dixit V S and Singh M 1998 *J. Mol. Spectrosc.* **187** 1
[19] Langhoff S R, Bauschlicher C W Jr and Taylor P R 1988 *J. Chem. Phys.* **88** 5715
[20] Brites V, Hammout'ene D and Hochlaf M 2008 *J. Phys. Chem. A* **112** 13419
[21] Bredohl H, Dubois I, Mahieu E and Mellen F 1991 *J. Mol. Spectrosc.* **145** 12
[22] Fleming P E and Mathews C W 1996 *J. Mol. Spectrosc.* **175** 31
[23] Hamade Y, Taher F and Monteil Y 2010 *Int. J. Quantum Chem.* **110** 1030
[24] Werner H J and Knowles P J 1985 *J. Chem. Phys.* **82** 5053
[25] Knowles P J and Werner H J 1985 *Chem. Phys. Lett.* **115** 259
[26] Werner H J, Knowles P J, Manby F R, Schutz M, Celani P, Knizia G, Korona T, Lindh R, Mitrushenkov A and Rauhut G *et al.* 2010 *Molpro* (Birmingham: University of Birmingham AL; see http://www.molpro.net.)
[27] Werner H J and Knowles P J 1988 *J. Chem. Phys.* **89** 5803
[28] Knowles P J and Werner H J 1988 *Chem. Phys. Lett.* **145** 514
[29] Langhoff S R and Davidson E R 1974 *Int. J. Quantum Chem.* **8** 61
[30] Douglas N and Kroll N M 1974 *Ann. Phys.* **82** 89
[31] Hess B A 1986 *Phys. Rev. A* **33** 3742
[32] Le Roy R J 2007 *LEVEL* 8.0*: A Computer Program for Solving the Radial Schrödinger Equation for Bound and Quasibound Levels, CPRR-661* (Waterloo: University of Waterloo, ON, Canada)
[33] Woon D E and Dunning T H Jr 1993 *J. Chem. Phys.* **98** 1358
[34] Peterson K A, Figgen D, Goll E, Stoll H and Dolg M 2003 *J. Chem. Phys.* **119** 11113
[35] Wyse F C and Gordy W 1972 *J. Chem. Phys.* **56** 2130
[36] Ram R S, Rai S B, Upadhya K N and Rai D K 1982 *Phys. Scr.* **26** 383
[37] Huber K P and Herzberg G 1979 *Molecular Spectra and Molecular Structure* (New York: Van Nostrand Reinhold)
[38] Griffith W B, J R and Mathews C W 1984 *J. Mol. Spectrosc.* **104** 347
[39] Rogowski D F and Fontijn A 1987 *Chem. Phys. Lett.* **137** 219